BNL-94441-2010-JA

Design of a 120 mm Bore 15 T Quadrupole for the LHC Upgrade Phase II

S. Caspi, G. Ambrosio, M. Anerella, E. Barzi, R. Bossert, D. Cheng, D. Dietderich, H. Felice, P. Ferracin, A. Ghosh, R. Hafalia, R. Hannaford, V. V. Kashikhin, D. Pasholk, G. L. Sabbi, J. Schmalzle, P. Wanderer, and A. Zlobin

***Abstract*—Future upgrades to machines like the Large Hadron Collider (LHC) at CERN will push accelerator magnets beyond 10 T forcing the replacement of NbTi superconductors with advanced superconductors such as Nb_3Sn. In support of the LHC Phase-II upgrade, the US LHC Accelerator Research Program (LARP) is developing a large bore (120 mm) Nb_3Sn Interaction Region (IR) quadrupole (HQ) capable of reaching 15 T at its conductor limit and gradients of 199 T/m at 4.4 K and 219 T/m at 1.9 K. The 1 m long, two-layer magnet, addresses coil alignment and accelerator quality features while exploring the magnet performance limits in terms of gradient, stress and structure. This paper summarizes and reports on the design, mechanical structure, coil windings, reaction and impregnation processes.**

***Index Terms*—HQ, LARP, Nb_3Sn, superconducting quadrupole magnet.**

I. Introduction

THE potential of reaching higher fields and gradients that go beyond existing magnets using NbTi technology made Nb_3Sn superconductors and it's more complex technology an attractive choice for future accelerator magnets. In the US three laboratories (BNL, FNAL, and LBNL) are collaborating to extend Nb_3Sn magnet technology into a design that demonstrates an option towards the fabrication of a full scale IR quadrupole magnet for the LHC Phase-II upgrade [1], [2]. In 2004 LARP started developing an IR quadrupole (TQ) that could reach 200 T/m in a 1 m long, 90 mm aperture [3], [4]. Over a dozen tests demonstrated that 200 T/m can be consistently achieved and exceeded. Although the current plateau never went beyond 95% of its "short-sample" prediction [5], a peak gradient of 237 T/m was reached at 1.9 K. The collaboration also demonstrated that the technology of 1 m long Nb_3Sn magnets can be extended to 3.6 m. A subscale racetrack coil was built and tested successfully reaching 98% of its "short-sample" limit [6]. LARP is presently weeks away from making a similar demonstration testing magnet LQS01 [7], [8], a 90 mm bore TQ quadrupole magnet that was extended from 1 m to 3.6 m long.

To meet CERN's Phase-II needs, LARP is also developing an IR quadrupole magnet (HQ) with an increased bore size of 120 mm which will push the field in the conductor to just over 15 T. This magnet will include accelerator features such as alignment and field quality. The HQ magnet Phase-II upgrade will operate at a gradient (yet to be determined) above CERN's Phase-I upgrade of 120 T/m [9], [10]. This paper covers the design parameters and the status of the HQ magnet.

Manuscript received October 13, 2009. First published February 18, 2010; current version published May 28, 2010. This work was supported by the Director, Office of Energy Research, Office of High Energy and Nuclear Physics, High Energy Physics Division, US Department of Energy under Contract DE-AC02-05CH11231.

S. Caspi, D. Cheng, D. Dietderich, H. Felice, P. Ferracin, R. Hafalia, R. Hannaford, and G. L. Sabbi are with Lawrence Berkeley National Laboratory, Berkeley, CA 94720 USA (e-mail: s_caspi@lbl.gov).

G. Ambrosio, E. Barzi, R. Bossert, V. V. Kashikhin, D. Pasholk, and A. Zlobin are with Fermi National Laboratory, Batavia, IL 60510-0500 USA.

M. Anerella, A. Ghosh, and P. Wanderer are with Brookhaven National Laboratory, Upton, NY 11973-5000 USA.

Color versions of one or more of the figures in this paper are available online at http://ieeexplore.ieee.org.

Digital Object Identifier 10.1109/TASC.2010.2040147

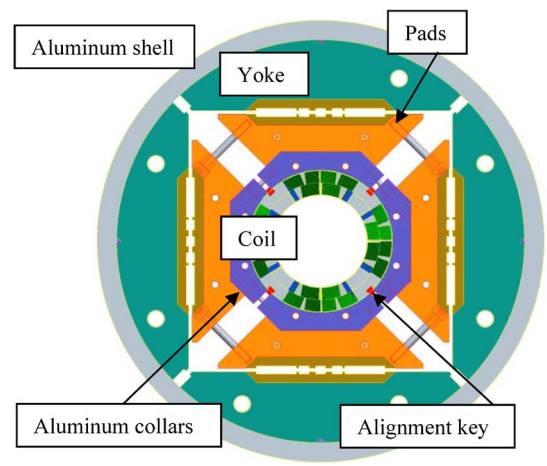

Fig. 1. HQ cross-section—120 mm high gradient Nb_3Sn quadrupole.

II. Magnet Design

A. HQ—Conceptual Design and Parameters

The cross-section of the HQ quadrupole magnet is shown in Fig. 1. The magnet components include: $cos2\theta$ coils, collars, pads, yokes and an outer shell. The effectiveness of the structural components was previously tested as part of the LARP TQ Nb_3Sn program with the exception of the collars [11], [12]. For the first time aluminum collars were incorporated into the design to provide alignment and assembly control but not for pre-stress [13].

The two layer coil uses a 35 strand Rutherford cable insulated with an S2 glass sleeve. The Nb_3Sn RRP strand diameter is 0.8 mm with 108/127 filament. Each layer of the double layer coil is wound around a Titanium pole (island) and includes stainless steel end-shoes and spacers. The stainless steel end pieces replaced previously used Bronze parts as a cost saving measure. A single Bronze wedge within each octant separates each

U.S. Government work not protected by U.S. copyright.

TABLE I
HQ DESIGNS PARAMETERS

Coil aperture	mm	120
Yoke OR	mm	260
Outer Shell thickness	mm	25
Overall magnet diameter	mm	570
Bare cable width	mm	15.15
Bare cable mid-thickness	mm	1.437
Cable keystone angle	deg	0.75
Cable insulation thickness	mm	0.10
Turns per quadrant IL/OL	t/m	20/26
Mid-plane shim per octant	mm	0.14
Maximum gradient 4.4 K/1.9 K	T/m	199/219
Maximum current 4.4 K/1.9 K	kA	17.7/19.5
Peak field 1.9 K	T	15.2
Peak field 4.4 K	T	13.9
Jc 12T, 4.2 K	A/mm^2	3000
Inductance (at quench)	mH/m	7.71
Max. stored energy 1.9 K	MJ/m	1.4
Max octant forces 1.9 K Fx total	MN/m	3.38
Max octant forces 1.9 K Fy total	MN/m	-5.03
Max octant forces 1.9 K F_θ IL/OL	MN/m	-1.92/-3.2
Maximum axial force per end	MN	1.4

TABLE II
CALCULATED HARMONICS OF HQ (IN UNITS)

Field reference radius		40mm
Harmonics @ 10 T/m	b_6	-1.63
	b_{10}	-0.01
	b_{14}	-0.01
	b_{18}	-0.39
Harmonics @ 120 T/m	b_6	0.00
	b_{10}	-0.00
	b_{14}	-0.01
	b_{18}	-0.41

layer into two blocks. The overall design parameters are listed in Table I.

B. Magnetic Design

The magnet was designed to reach a "short-sample" field, gradient and current of 15.2 T, 219 T/m and 19.5 kA respectively at 1.9 K (based on Jc of 3000 A/mm^2 at 4.2 K 12 T). The good field quality at 2/3 of the bore radius was set at a gradient of 120 T/m. Table II lists the first 4 allowed harmonics at low and intermediate field.

The load pad laminations at the end regions were replaced with stainless steel to reduce the conductor end peak field to the same level as that of the straight section. The integrated field quality over the ends will be addressed at a future date.

C. Quench Protection

A quench analysis has been performed using the program QuenchPro [14]. The analysis evaluated the expected peak temperature in the coil (hot spot temperature) after a spontaneous quench. With a stored energy of 1.4 MJ, wide protection heaters are needed for both layers. The protection heaters are part of a trace: an instrumentation technique adopted in all LARP magnets relying on printed-circuit technology and based on a Kapton sheet and a 25.4 microns thick stainless steel foil [15]. A 65% heater coverage and a conservative approach (low quench propagation velocity and no quench-back) result in a hot spot temperature of around 300 K for a short sample quench at 4.4 K but reaches ~400 K at a short sample current at 1.9 K. We consider such a rise in temperature unacceptable, nevertheless given the limited number of options the degree of our conservative approach will need to be experimentally evaluated.

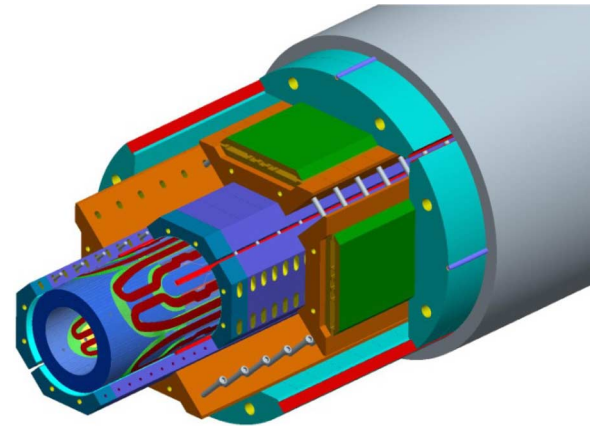

Fig. 2. Final assembly of coils and structure.

D. Assembly and Cool-Down

The coil-pack subassembly consists of four aluminum collars that are clamped and bolted over the coils and align the coils by compressing four keys between them (Fig. 1). The keys are embedded in each coil's outer layer island/pole. The collars are used for assembly and alignment only and not to provide pre-stress as commonly used in NbTi magnets. Surrounding the faceted collars are four steel pads with matching facets. The pad-quadrants are lightly bolted to each other completing the coils subassembly.

A second subassembly is the structure which consists of an iron yoke and an aluminum shell. The shell and yoke are locked together following a bladder operation that stretches the outer shell by pushing the inner iron yoke against it. During this operation, alignment dowels are inserted in precision-machined grooves between the yokes and the shell inner surface in four places. Interference "gap-keys" are placed between the yokes to lock, unitize and preload the subassembly.

During the final assembly, the coil-pack assembly is inserted into the shell-yoke structure on faceted "master keys" (an alignment feature) which engage matching profiles in both coil-pack and yoke structures. Bladders and interference load keys (Figs. 1 and 2) are inserted between the master keys. Bladder pressurization operations are performed to, outwardly, push the yokes (to stretch the shell) and, inwardly, compress the coil-pack. Once the target azimuthal strain on the instrumented shell is attained, the load keys are interference shimmed. The bladders are deflated and removed along with the gap keys, collapsing and locking the shell-yoke structure onto the keys and coil pack. The tension in the outer aluminum shell is now balanced by the azimuthal compressive stress in the coils. The final coil pre-stress is achieved during cool-down as the aluminum shrinks over the yoke and pads due to the thermal expansion differences between the two.

TABLE III
AVERAGE AZIMUTHAL STRESS

Location	σθ BO (MPa)	σθ CD (MPa)	σθ LF (MPa)
Layer 1 Island	-68	-160	+54
Layer 2 Island	-23	-49	+33
Layer 1 pole-turn	-48	-140	-7
Layer 2 pole-turn	-24	-78	+9
Outer Shell	+100	+210	+214

TABLE IV
AVERAGE AZIMUTHAL STRAIN

Location	εθ BO (μs)	εθ CD (μs)	εθ LF (μs)
Layer 1 Island	-484	-790	+699
Layer 2 Island	-148	-55	+486
Layer 1 pole-turn	-993	-3423	-652
Layer 2 pole-turn	-509	-2098	-298
Outer Shell	+1302	+2363	+2412

TABLE V
AVERAGE AXIAL STRESS

Location	σz BO (MPa)	σz CD (MPa)	σz LF (MPa)
Layer 1 Island	-18	-163	-90
Layer 2 Island	-6	-128	-91
Layer 1 pole-turn	-10	+18	+50
Layer 2 pole-turn	-5	+30	+53
Outer Shell	+25	+67	+70
Axial Rods (σz)	+93	+191	+205

TABLE VI
AVERAGE AXIAL STRAIN

Location	εz BO (μs)	εz CD (μs)	εz LF (μs)
Layer 1 Island	+14	-823	-740
Layer 2 Island	+13	-828	-742
Layer 1 pole-turn	+14	+785	+870
Layer 2 pole-turn	+14	+786	+870
Outer Shell	-132	-49	-39
Axial Rods	+1323	+2416	+2592

E. Mechanical Analysis

2D and 3D Finite Element Analysis were performed with ANSYS to predict the stresses in the windings and structure. The analyses were done in 3 steps a) during room temperature loading (bladder operation BO), b) cool-down (CD) and c) excitation (LF). Tables IIIto VI summarize the average stress and strain in the coil-island, coil pole turn, shell and axial rods from assembly to 219 T/m. A maximum local stress of 209 MPa was predicted after cool-down in layer 1 third turn from the island. Such a local high stress was previously predicted in TQ with minimum impact on its performance.

III. HQ COILS

A. Practice Coil—Winding Test

Preliminary winding tests were carried out to determine the cable lay around the ends. The islands, spacers, end-shoes and wedges used in the tests were made from plastic rapid-prototype (RP) parts (Fig. 3). The RP parts were manufactured directly from CAD ProE models and included various holes and the layer-to-layer transition. The use of RP parts during magnet design proved to be very useful and cost effective.

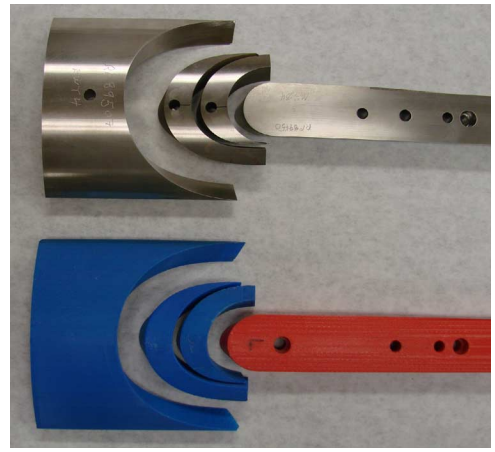

Fig. 3. Lead end components using RP parts (bottom), Stainless-Steel parts (top) and Titanium island.

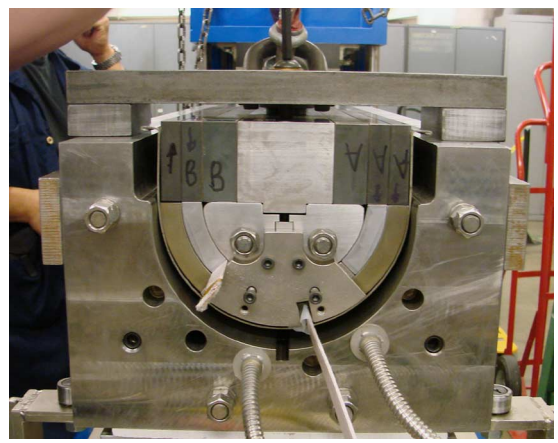

Fig. 4. Inserting PC 1 into the curing cavity. The process sizes the coils, bonds the turns and makes coil handling more manageable.

Fig. 5. The bound inner layer of coil 3 after curing.

B. Coil Fabrication

Winding Nb3Sn coils undergoes several steps: winding, curing, reacting, impregnating and require 3 sets of different tooling. Following the winding of the first layer (inner) the coil is treated with a matrix solution and placed inside a curing cavity, pre-sized under 11 MPa of compression and cured at 150°C. The curing process bonds the turns together, shapes the overall coil size and creates a uniform outer surface on to which the outer layer can then be wound (Figs. 4 and 5). Completing the second layer winding the coil is treated again with the matrix solution, placed once again into the curing cavity, aligned and cured. After curing the preset 0.7 mm axial gap between island segments (administered by the winding tooling) is removed, the gap closes and the coil relaxes its winding tension. The coil is then placed into a reaction cavity (Fig. 6) and reacted at 665°C following intermediate temperature steps at 210°C and 400°C. The reaction time from start to finish is approximately 10 days.

Fig. 6. PC1 inside reaction tooling ready for reaction.

Fig. 7. Lead end of practice coil 2 showing NbTi leads after splicing. Also shown are voltage taps and layer 2 heaters.

Fig. 8. Impregnated coil showing the inner layer trace and the protection heater.

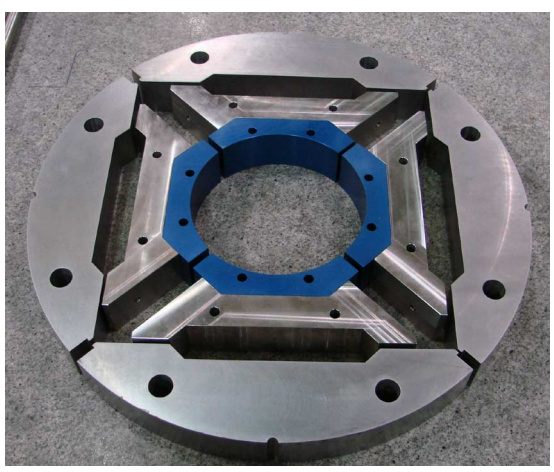

Fig. 9. A set of the structure laminations showing the outer iron yoke, the iron pads and Aluminum collars. The space between yoke and pads will house the masters that hold the bladders and interference keys.

Following reaction, voltage taps (installed during winding) are attached to instrumentation traces that include the integrated coil protection heaters. The Nb_3Sn to NbTi lead splice is soldered (Fig. 7) and the coil is placed into the impregnated tooling and then vacuum impregnated with CTD101k epoxy (Fig. 8). After impregnation two full bridge (temperature compensated) strain gauges are bonded to the inner surface of the island at the magnet center to measure and determine the azimuthal and axial coil stress.

All coils are being wound and cured at LBNL. Half of the coils are then reacted and impregnated at LBNL and the second half is sent for reaction and impregnated at BNL Design and manufacturing of all end parts, islands and wedges are taken care of by FNAL.

C. Structure

All the structure components have been manufactured and waiting assembly (Fig. 9). The plan is to complete the structure assembly with an aluminum dummy coil-pack and align the iron yokes to the aluminum shell.

IV. Future Plans

Presently two impregnated practice coils (PC-1, 2) have been completed and two reacted coils (Coil-3 and Coil-4) are waiting reaction. Four coils (Coils-3 to 6) will be used in the first HQ01 magnet test. Assembly will commence in early 2010 and testing shortly after.

V. Conclusion

The manufacturing of the first four coils for a large aperture (120 mm, 219 T/m at 1.9 K) quadrupole magnet (HQ) is near completion. The sub-assemblies of the structure and coils and the final assembly will take place in early 2010.

Acknowledgment

The authors thank the technical staff of BNL, FNAL and LBNL for their professional work and dedication to the HQ program.

References

[1] S. A. Gourlay *et al.*, "Magnet R&D for the LHC accelerator research program," *IEEE Trans. Appl. Supercond.*, vol. 16, no. 2, pp. 324–327, June 2006.
[2] P. Wanderer *et al.*, "Overview for LARP magnet R&D," *IEEE Trans. Appl. Supercond.*, vol. 19, no. 3, pp. 1208–1211, June 2009.
[3] S. Caspi *et al.*, "Test results of LARP Nb3Sn quadrupole magnets using a shell-based support structure (TQS)," *IEEE Trans. Appl. Supercond.*, vol. 19, no. 3, pp. 1221–1225, June 2009.
[4] B. Bossert *et al.*, "Fabrication and test of LARP technological quadrupole models of TQC series," *IEEE Trans. Appl. Supercond.*, vol. 19, no. 3, pp. 1226–1230, June 2009.
[5] H. Felice *et al.*, "Test results of TQS03: A LARP shell-based Nb_3Sn quadrupole using 108/127 conductor," in *9th European Conf. on Appl. Supercond.*, Dresden, Germany, Sept. 2009, to be published.
[6] P. Wanderer *et al.*, "Construction and test of a 3.6 m Nb_3Sn racetrack coils for LARP," *IEEE Trans. Appl. Supercond.*, vol. 18, no. 2, pp. 171–174, June 2008.
[7] P. Ferracin *et al.*, "Fabrication and test of a 3.7 m long support structure for the LARP Nb_3Sn quadrupole magnet LQS01," *IEEE Trans. Appl. Supercond.*, vol. 19, no. 3, pp. 1106–1111, June 2009.
[8] G. Ambrosio *et al.*, "Development and coil fabrication for the LARP 3.7-m long Nb_3Sn quadrupole," *IEEE Trans. Appl. Supercond.*, vol. 19, no. 3, pp. 1231–1234, June 2009.
[9] R. Ostrojic, "LHC interaction region upgrade—Phase I," LHC PR 1094, August 2008.
[10] P. Fessia *et al.*, "Design of a 120 mm bore quadrupole for the LHC upgrade phase I," paper 1AO-04 this conference.
[11] S. Caspi *et al.*, "Mechanical design of a second generation LHC IR quadrupole," *IEEE Trans. Appl. Supercond.*, vol. 14, no. 2, pp. 235–238, June 2004.
[12] A. R. Hafalia *et al.*, "Structure for an LHC 90 mm Nb_3Sn quadrupole magnet," *IEEE Trans. Appl. Supercond.*, vol. 15, no. 2, pp. 1444–1447, June 2005.
[13] H. Felice *et al.*, "Design of HQ-A high field large bore Nb_3Sn quadrupole magnet for LARP," *IEEE Trans. Appl. Supercond.*, vol. 19, no. 3, pp. 1235–1239, June 2009.
[14] P. Bauer *et al.*, "Concept for a quench calculation program for the analysis of quench protection systems for superconducting high field magnets," FNAL TD Notes TD-00-027.
[15] H. Felice *et al.*, "Instrumentation and quench protection for LARP Nb3Sn magnets," *IEEE Trans. Appl. Supercond.*, vol. 19, no. 3, pp. 2458–2462, June 2009.